ELSEVIER

Carbohydrate Research 266 (1995) 15–35

CARBOHYDRATE RESEARCH

On the conformational and packing behaviour of acyclic sugar amphiphiles: the crystal structures of *N*-(1-octyl)-D-arabinonamide and *N*-(1-dodecyl)-D-ribonamide and the supramolecular assembly-forming properties of *N*-(1-octyl)-D-pentonamides

Christoph André [a,*], Peter Luger [a], Reinhard Bach [b], Jürgen-Hinrich Fuhrhop [b]

[a] *Institut für Kristallographie, Freie Universität Berlin, Takustr. 6, 14195 Berlin, Germany*

[b] *Institut für Organische Chemie, Freie Universität Berlin, Takustr. 3, 14195 Berlin, Germany*

Received 9 February 1994; accepted in revised form 6 July 1994

Abstract

The crystal structure of *N*-(1-octyl)-D-arabinonamide [space group $P2_1$, $a=4.855(3)$ Å, $b=30.45(3)$ Å, $c=10.59(1)$ Å, $\beta=94.46(6)°$] shows two independent molecules arranged in an antiparallel manner in the asymmetric unit. Their head groups and octyl chains are extended, but the overall shape of the molecules is different. The packing arrangement in the crystal, with interdigitating head groups and oligomethylene tails, has never been observed before with aldonamides, but is identical with that of the glucitol amphiphile MEGA-8. Comparison of the packing of the arabinonamide molecules in the crystal with that of other amphiphiles crystallizing in an antiparallel arrangement reveals a similar behaviour, suggesting a common mechanism of crystallization for these compounds. *N*-(1-Dodecyl)-D-ribonamide [space group $P1$, $a=4.815(2)$ Å, $b=5.464(2)$ Å, $c=18.084(4)$ Å, $\alpha=81.77(2)°$, $\beta=87.78(3)°$, $\gamma=83.83(3)°$] displays one molecule in the asymmetric unit. It exhibits two straight-chain segments from C-2 to C-5 and C-2 to C-14, respectively, and shows an unexpected 1,3-syndiaxial interaction between C-1, the carbonyl carbon atom, and O-4. The hydrogen-bond patterns involve a quadrilateral homodromic cycle between between four molecules related by translation along the two 5 Å axes. The molecular packing is head-to-tail as observed in the crystal structures of amphiphilic gluconamides displaying an analogous homodromic cycle. It has been shown earlier that *N*-octyl-D-gluconamide forms solid micellar fibers in water, whereas the analogous ribose derivative investigated in this paper forms planar bilayer sheets instead of micellar threads, although the molecular interactions in the crystal sheets are similar to those in gluconamide. *N*-Octyl-D-arabinonamide, on the other hand, forms ill-defined tubular bilayers.

* Corresponding author.

SSDI 0008-6215(94)00260-6

Keywords: Amphiphiles, acyclic sugar; Conformational behaviour; Packing behaviour; Crystal structure; Arabinonamide, *N*-(1-octyl)-D-; Ribonamide, *N*-(1-dodecyl)-D-

1. Introduction

The properties of amphiphiles having acyclic sugar head groups have been intensely investigated during past years. After Pfannemüller and Welte found that *N*-(1-alkyl)-D-gluconamides form thick helical ropes after cooling down their aqueous solutions [1], the propensity of hexonamides to form supramolecular assemblies was thorougly studied in order to test the aptitude of these structures as scaffoldings for biomimetic reactions and to understand the mechanistic relationship between the configuration of the head group and the superstructures formed [2–7]. It has been found, for example, that *N*-octyl-D-gluconamide forms micellar threads in water which assemble to form solid quadruple helices. The diameter of the threads was 3.9 nm, thus corresponding exactly to a circular molecular bilayer. The diastereomeric *N*-octyl-D-mannonamide, on the other hand, formed planar molecular bilayers instead of micellar threads. Small differences in stereochemistry (only the chiral center at C-2 had changed) thus caused enormous differences in the appearance of supramolecular assemblies. The gluconamide assembly's curvature has been traced back to (*i*) a 1,3-sterical repulsion between OH-groups in syndiaxial positions, (*ii*) a homodromic hydrogen-bond cycle, and (*iii*) an unfavorable rearrangement of the tail-to-tail ordering of molecules in the fiber as compared to head-to-tail in the crystals. None of these three effects was observed in the corresponding mannonamide platelets. We have now performed the corresponding experiments with analogous pentonamides, namely *N*-(1-octyl)-D-arabinonamide (**1**), where no ecliptic OH-groups in 1,3-positions of the extended carbohydrate chains are present, and *N*-(1-octyl)-D-ribonamide (**3**), where such an arrangement occurs. Since the glucon- and the ribon-amide both exhibit two OH-groups in 1,3-syndiaxial disposition, whereas the mannon- and arabinon-amide lack such an arrangement, it was expected, that **3** would form fibers, whereas **1** should form superstructures without any curvature. It will be shown, that these simple extrapolations on the supramolecular behaviour are *not* valid.

Until recently, it was widely accepted that the avoidance of O//O- and C//O-interactions, namely parallel C_n–O–/C_{n+2}–O– or C_n–O–/C_{n+2}–C bonds, was the primary factor determining the conformation of open-chain sugar derivatives in the solvated and crystalline states [8]. However, the validity of this so-called Hassel–Ottar effect [9] for acyclic systems was challenged by the finding of many unexpected O//O- and C//O-interactions in the crystal structures of alditols and nitro-alditols (compare Ref. [10] and references cited therein).

This work is part of our studies on amphiphilic aldonamides, which have included thus far the crystal structures of *N*-(1-octyl)-D-gulonamide [11], the corresponding talose derivative [12], *N*alkanediylgluconamides [13,14], and the double-headed (1*S*,2*S*)-1,2-bis(D-gluconamido)cyclohexane [15]. Systematic studies on these amphiphiles are especially interesting since they give insight into the interplay of conformational and packing behaviour of substances with many possible intermolecular hydrogen bonds, thereby providing information on crystallization of organic compounds in general. Herein, we report on the crystal

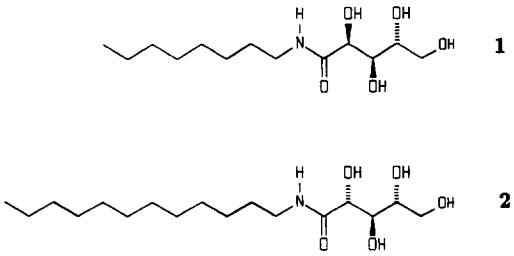

Scheme 1.

structures of *N*-(1-octyl)-D-arabinonamide (**1**) and *N*-(1-dodecyl)-D-ribonamide (**2**). Apart from the *per se* undisturbed DL-*erythro*-1,2,3-heptanetriol [16] and D-*erythro*-2-acetamido-1,3-diacetoxy-4-*trans*-octadecene [17], the arabinonamide is the first crystal structure of an amphiphilic open-chain sugar derivative without O//O-interactions in its head group (Scheme 1).

2. Experimental

Preparation of N-*octyl*-D-*arabinonamide* (**1**).—D-(−)-Arabinose (3 g, 20 mmol) was dissolved in 75 mL of water containing 0.6 g (3 mmol) of $CaBr_2$ and 4 g (40 mmol) of $CaCO_3$. The mixture was electrolyzed with carbon electrodes with a current of 200 mA [18]. Oxidation to the lactone was terminated after 320 min, $CaCO_3$ was filtered off, and the solution was stirred with 10 g of acidic ion-exchange resin (Merck, Type 1). The resin was removed by filtration, and the filtrate was passed into a suspension of 1.24 g (4.5 mmol) of Ag_2CO_3 in 25 mL of water, to precipitate bromide and carbonate. The mixture was filtered with a membrane filter (Sartorius, pore width 0.2 μm) and the filtrate chromatographed on an acidic ion-exchange column (Merck, Type 1). The column was eluted with water until the eluate was neutral, and the eluate was evaporated. The resulting oily arabinolactone (4.4 g, 20 mmol) was dissolved in MeOH and refluxed for 1.5 h with 2.59 g (20 mmol) of octylamine. Crystallization overnight at −21°C, and two recrystallizations from MeOH, gave 4.1 g (74%) of white crystallites of **1**; mp 156–158°C. Anal. Calcd for $C_{13}H_{27}NO_5$ (277.19): C, 56.30; H, 9.81; N 5.05. Found: C, 56.25; H, 9.94; N, 4.75. Spectral data [(^{1}H NMR, IR, EIMS (80 eV)] were according to expectation]. Very slow evaporation (ca. 4 months) from Me_2SO yielded a tiny, needle-shaped crystal of **1**.

The procedure for *N*-octyl-D-ribonamide (**3**) was identical to that just described, but from D-ribose (3 g) [yield 3.4 g (62%)]; mp 98–99°C. Anal. Found: C, 56.08; H, 10.00; N, 4.98.

The other two diastereomeric *N*-octyl-D-pentonamides having D-*lyxo* (2*R*,3*S*,4*R*) and D-*xylo* (2*R*,3*S*,4*S*) configurations were also prepared, as well as the *N*-dodecyl-D-ribonamide (**2**). All compounds gave satisfactory analyses and spectral data. Single crystals of **2** of good quality could readily be grown by evaporation from a solution in 1:1 acetone–H_2O. However, we were not able to obtain good crystals from the xylon- and lyxon-amides.

DSC measurements of the gels and the powders of the pentonamides were performed with a Perkin–Elmer DSC-2C differential scanning calorimeter with a heating rate of 2.5°C/min (gels) and 1.25°C/min (powders).

Table 1
XPLOR-refinement of **1**

Protocol
All hydrogen atoms treated explicitely by using the XPLOR-parameter set PARMALLH3x.PRO
Charges taken from PARMALLH3x.PRO
Optimization of bond lengths, angles, torsion angles, Van der Waals and Coulomb interactions (12-6-1-potential), and hydrogen bonds; inclusion of improper terms in order to maintain correct chirality at C-2, C-3, and C-4 in both independent molecules
Simulated-annealing simulation started at 3000 K and decreased every 50 dynamic steps by 25 K to a final temperature of 300 K (Verlet-integration algorithm with a time step of 0.5 fs)
Average difference of atomic positions before/after the XPLOR-optimization 0.2(1) (esd in parentheses)

Crystal-structure analysis.—The determination of the space groups was performed after visual inspection of the Weissenberg exposures from which preliminary lattice constants were taken. Refinement of the lattice constants and measurement of the intensity data was performed for both compounds at room temperature on a Stoe four-circle diffractometer with Ni-filtered Cu$K\alpha$ radiation in the $\omega-2\Theta$ scan mode.

Compound **2** was solved readily by direct methods using SHELXS-86 [19] with the *E*-map displaying all nonhydrogen atoms. All hydrogen atoms of **2** were located after anisotropic refinement of this model and were included with isotropic temperature parameters in the final refinement cycles. All atom parameters, except H-1N, H-182, and the temperature factor of HO-3 which were held fixed, could be refined with XTAL 2.2 [20] to convergence to a final *R*-value of 0.045 ($R_w = 0.048$).

SHELXS-86 failed to solve the structure of **1** since 65% of the measured reflections were unobserved. It could only be solved by MITHRIL [21] after an *arabino*-configured headgroup fragment had been introduced for molecular scattering-factor calculation. As **1** crystallizes in the $P2_1$ space group and four molecules had been calculated for the unit-cell content, two independent molecules were expected for the asymmetric unit. Subsequently two molecular fragments (C-5 to O-1 and C-5A to C-8A) exhibiting poor geometrical values could be found after intense interpretation of the diffuse *E*-map generated by MITHRIL. It is remarkable that this structure solution was obtained with only 30% of the measured reflections. All missing carbon atoms of the octyl chains were located in difference-Fourier maps calculated after some cycles of isotropic refinement using XTAL 2.2. Interpretation of these maps was mainly directed by the search for peaks in the all-*trans* conformation expected for aliphatic chains, since their bond lengths and angles indicated rather bad geometry. After four cycles of weighted isotropic refinement, the weighted *R*-value dropped to 0.108, whereas the unweighted *R*-value remained at 0.201. To improve the geometry of the model, the final refinement was performed using the computer program XPLOR 3.0 [22] which is described in detail in Ref. [23]. It performs a geometry optimization by simulated annealing [24] involving experimental structure factors, intermolecular interactions, and other factors, as restraints. A short protocol of the XPLOR-refinement is given in Table 1; more-detailed information, including the energy parameters of the geometrical optimization, has been deposited.

After the XPLOR-refinement, the *R*-value was 0.217 (weighted *R*-value = 0.123) which is only a minor deterioration to the input value; the geometry of the molecules, however, had been considerably improved. This poor *R*-value must mainly be attributed to the low

Table 2
Crystallographic data of **1** and **2**

Compound	**1**	**2**
Formula	$C_{13}H_{27}NO_5$	$C_{17}H_{35}NO_5$
Molecular weight	277.36	333.47
Crystal size (mm)	0.30×0.04×0.005	0.80×0.38×0.20
T (K)	295	295
Space group	$P2_1$	$P1$
Z	4	1
Lattice constants		
a (Å)	4.855(3)	4.815(2)
b (Å)	30.45(3)	5.464(2)
c (Å)	10.59(1)	18.048(4)
α (°)	(90)	81.77(2)
β (°)	94.46(6)	87.78(3)
γ (°)	(90)	83.83(3)
Cell volume (Å^3)	1560.3	467.1
D_x (g/cm^3)	1.181	1.186
Absorption coefficient		
μ (cm^{-1})	7.46	7.03
Radiation used	Cu$K\alpha$	Cu$K\alpha$
$2\Theta_{max}$ (°)	100	128
Total number of symmetry-independent reflections	1642	1499
$F<2\sigma(F)$	1054	13
w in refined sum $\Sigma w(\lvert F_o\rvert - \lvert F_c\rvert)^2$	$1/\sigma^2$	$1/\sigma^2$
R	0.217	0.045
R_w	0.123	0.048

number of observed reflections, which only permitted an isotropic refinement with an arbitrary temperature-factor. We consider, however, that the general packing scheme and the conformation of the molecules of **1** have been unambiguously solved.

Table 2 displays the crystal and refinement data for **1** and **2**. Table 3 gives DSC data of *N*-(1-octyl)-D-pentonamides and some related compounds. The atomic coordinates of **1**

Table 3
DSC data for *N*-(1-octyl)-D-pentonamides and some related compounds [a]

Compound	T	ΔH	T	ΔH	T	ΔH	Range of measurement [b]
1					158	54.0	47–177 [c]
DLyx8			111	44.9	12.6	2.9	27–207
DXyl8	40	19.3	91	11.5	133	2.4	27–167
3	94	53.1	118	1.7			27–187
3 [d]	96		123				
DRib10 [e]	99	67.9	151	1.6			
2	99	14.7	103	45.9			47–207
2 [d]			105		160		

[a] T in °C, ΔH in kJ mol^{-1}. [b] In °C. [c] No further peak at higher temperatures observable. [d] Taken from Ref. [27] where no ΔH-values were given. [e] Taken from Ref. [28].

Table 4
Fractional atomic coordinates of **1**

Atom	*x*	*y*	*z*
C-1	−0.003	0.0397	−0.117
O-1	−0.119	0.0231	−0.031
C-2	0.201	0.0768	−0.086
H-2	0.346	0.0656	−0.011
O-2	0.335	0.0923	−0.195
HO-2	0.211	0.1169	−0.216
C-3	0.028	0.1159	−0.036
H-3	−0.085	0.1046	0.041
O-3	−0.148	0.1307	−0.142
HO-3	−0.342	0.1219	−0.139
C-4	0.201	0.1563	0.003
H-4	0.297	0.1675	−0.080
O-4	0.408	0.1449	0.100
HO-4	0.348	0.1193	0.145
C-5	0.023	0.1934	0.057
O-5	−0.092	0.1769	0.170
HO-5	−0.294	0.1772	0.151
N-1	−0.040	0.0285	−0.237
HN-1	0.070	0.0456	−0.293
C-7	−0.226	−0.0061	−0.289
C-8	−0.066	−0.0417	−0.353
C-9	−0.268	−0.0703	−0.435
C-10	−0.127	−0.1052	−0.513
C-11	−0.343	−0.1311	−0.591
C-12	−0.200	−0.1665	−0.668
C-13	−0.424	−0.1934	−0.743
C-14	−0.293	−0.2294	−0.818
C-1A	0.010	0.1667	0.520
O-1A	0.014	0.1692	0.637
C-2A	0.183	0.1312	0.459
O-2A	0.365	0.1120	0.556
HO-2A	0.221	0.1103	0.617
C-3A	−0.009	0.0927	0.413
O-3A	−0.123	0.0733	0.522
HO-3A	−0.315	0.0826	0.527
C-4A	0.171	0.0550	0.355
O-4A	0.301	0.0733	0.249
HO-4A	0.498	0.0654	0.261
C-5A	−0.008	0.0171	0.308
O-5A	−0.205	0.0365	0.218
HO-5A	−0.169	0.0256	0.135
N-1A	−0.135	0.1922	0.441
H-1NA	−0.127	0.1876	0.350
C-7A	−0.311	0.2271	0.490
C-8A	−0.467	0.2510	0.383
C-9A	−0.267	0.2801	0.313
C-10A	−0.437	0.3083	0.217
C-11A	−0.254	0.3426	0.161
C-12A	−0.432	0.3706	0.068
C-13A	−0.241	0.4043	0.016
C-14A	−0.412	0.4349	−0.074

and **2** are listed in Tables 4 and 5[1]. Bond lengths and angles of **2** are shown in Table 6, and relevant torsion angles of **1** and **2** and related compounds are given in Tables 7 and 8. The hydrogen-bond geometry of the title compounds is shown in Tables 9 and 10, respectively.

3. Results and discussion

Supramolecular assemblies and DSC measurements.—The four pentonamides did not dissolve in cold water. At 100°C the *N*-octylarabinonamide dissolved to ca. 2%, the other three pentonamides to ca. 50%! In order to investigate gelation and fiber formation, 40 mg of the pentonamides were each dissolved in 40 mL of boiling water and cooled to 5°C. The arabinonamide (**1**) gave a white gel that was stable for several days. The gel slowly shrank and finally yielded long white needles (Fig. 1a). Electron micrographs of the gel show thick rods (diameter = 100 nm; not shown). *N*-Octyl-D-lyxonamide behaved similarly. *N*-Octyl-D-xylon- and ribon-amide **3**, on the other hand, formed no long-lived gels. They precipitated as platelets, which could be identified as molecular bilayers under the electron microscope (Fig. 1b). Thermo-differential analysis (DSC) of the gels gives relatively broad-melting peaks at 94°C (*arabino*), 63°C (*lyxo*), and 34°C (*ribo*) for the *N*-octylpentonamides. D-Xylonamide gave no signal in the range between 5 and 80°C. No micellar threads could be obtained from any of the *N*-octylpentonamides. The sharp bend in the molecular structure of the ribonamide (see later) obviously prevents a stable assembly having a circular or helical arrangement. This is another example for Kunitake's old statement on supramolecular assemblies saying, "Too much bending is not advantageous for molecular ordering" [25].

On heating the powder samples, DSC measurements revealed two phase transitions for **2**, **3**, and the lyxonamide; **1** displayed only one phase transition whereas three were observed for the xylonamide. The thermotropic behaviour of open-chain sugar amphiphiles is dominated by the occurrence of smectic phases; in fact, octyl-, decyl-, and dodecyl-ribonamide have previously been shown to form a smectic A_d mesophase [26,27]. Our data for **2** are generally in agreement with the results of Baeyens-Volant et al. [27]. However, we did not detect the phase transition at 160°C reported for **3**, whereas we found a phase transition at 99°C that was not reported in the previous study [27].

Crystal structures.—Molecular structure. The molecular geometry and the numbering scheme of the independent molecules in the asymmetric unit of **1** are displayed in Fig. 2. Since the final structure of **1** is the result of a simulated-annealing-calculation rather than of a conventional crystallographic refinement, no esd's can be given for the coordinates of **1** and consequently for the geometry of it.

Both sugar segments display an extended conformation – as may be expected for a sugar undisturbed by 1,3-syndiaxial interactions, with the terminal hydroxyl groups O-5 and O-

[1] A complete atom list, including the hydrogen atom and displacement parameters for **1**, together with the list of observed and calculated structure factors for **1** and **3** and details of the XPLOR-refinement of **3** can be obtained on request from the Director, Cambridge Crystallographic Data Centre, 12 Union Road, Cambridge CB2 1EZ, United Kingdom.

Table 5
Fractional atomic coordinates and equivalent isotropic temperature factors U_{eq} ($Å^2 \times 10^2$) of **2**

Atom	x	y	z	U_{eq} [a]
C-1	−0.83470(-)	0.00540(-)	0.79380(-)	3.4(1)
O-1	−0.582(1)	−0.005(1)	0.8031(3)	4.4(1)
C-2	−0.955(1)	−0.156(1)	0.7418(4)	3.4(1)
H-2	−1.097(9)	−0.237(9)	0.772(3)	3(1)
O-2	−0.733(1)	−0.325(1)	0.7196(3)	3.8(1)
HO-2	−0.80(1	−0.406(9)	0.699(3)	3(1)
C-3	−1.116(1)	−0.010(1)	0.6750(4)	3.3(1)
H-3	−1.244(9)	0.108(8)	0.689(3)	3(1)
O-3	−1.267(1)	−0.175(1)	0.6417(3)	4.1(1)
HO-3	−1.39(1)	−0.22(1)	0.672(3)	4.6(-)
C-4	−0.932(1)	0.111(1)	0.6120(4)	3.6(1)
H-4	−0.77(1)	−0.02(1)	0.599(3)	6(2)
O-4	−0.786(1)	0.2837(9)	0.6439(3)	4.0(1)
HO-4	−0.70(2)	0.36(2)	0.611(5)	10(3)
C-5	−1.099(1)	0.242(1)	0.5455(4)	4.2(2)
H-51	−0.98(1)	0.32(1)	0.503(3)	5(1)
H-52	−1.19(1)	0.08(1)	0.521(3)	5(1)
O-5	−1.315(1)	0.419(1)	0.5652(3)	4.3(1)
HO-5	−1.24(1)	0.54(1)	0.581(3)	6(2)
N	−1.024(1)	0.143(1)	0.8284(3)	3.9(1)
H-N	−1.214(-)	0.16(-)	0.824(-)	4.4(-)
C-7	−0.940(1)	0.293(1)	0.8837(4)	4.0(1)
H-71	−0.819(9	0.424(9)	0.850(3)	4(1)
H-72	−0.832(9)	0.192(9)	0.922(3)	4(1)
C-8	−1.187(1)	0.428(1)	0.9196(4)	4.1(1)
H-81	−1.32(1)	0.31(1)	0.947(4)	8(2)
H-82	−1.30(1)	0.53(1)	0.879(3)	5(1)
C-9	−1.088(1)	0.578(1)	0.9766(4)	4.5(2)
H-91	−0.964(8)	0.714(8)	0.946(2)	3(1)
H-92	−0.98(1)	0.481(9)	1.008(3)	4(1)
C-10	−1.321(1)	0.723(1)	1.0156(4)	4.7(2)
H-101	−1.48(1)	0.64(1)	1.038(3)	6(2)
H-102	−1.41(1)	0.87(1)	0.972(3)	7(2)
C-11	−1.213(1)	0.860(1)	1.0752(4)	4.9(2)
H-111	−1.09(1)	0.978(9)	1.045(3)	4(1)
H-112	−1.09(1)	0.756(9)	1.109(3)	5(1)
C-12	−1.439(1)	1.011(1)	1.1154(4)	5.1(2)
H-121	−1.57(2)	0.92(1)	1.136(4)	9(2)
H-122	−1.56(1)	1.15(1)	1.074(3)	6(2)
C-13	−1.325(1)	1.141(1)	1.1753(4)	5.2(2)
H-131	−1.19(1)	1.04(1)	1.211(3)	5(1)
H-132	−1.22(1)	1.264(9)	1.143(3)	5(1)
C-14	−1.542(1)	1.295(1)	1.2170(4)	5.6(2)
H-141	−1.64(1)	1.46(1)	1.172(4)	11(3)
H-142	−1.67(1)	1.22(1)	1.232(3)	5(2)
C-15	−1.419(1)	1.419(1)	1.2765(5)	5.7(2)
H-151	−1.29(1)	1.54(1)	1.246(4)	7(2)
H-152	−1.31(1)	1.32(1)	1.312(3)	5(1)
C-16	−1.633(1)	1.577(1)	1.3196(4)	5.8(2)

Table 5 (continued)

Atom	x	y	z	U_{eq} [a]
H-161	−1.75(1)	1.46(1)	1.350(4)	8(2)
H-162	−1.72(1)	1.70(1)	1.279(4)	7(2)
C-17	−1.497(2)	1.699(2)	1.3774(5)	7.3(2)
H-171	−1.39(1)	1.58(1)	1.417(4)	9(2)
H-172	−1.37(1)	1.82(1)	1.338(4)	7(2)
C-18	−1.706(2)	1.856(2)	1.4211(5)	8.5(3)
H-181	−1.83(2)	1.95(1)	1.389(4)	10(3)
H-182	−1.88(2)	1.75(2)	1.456(5)	9.9(-)
H-183	−1.61(1)	1.94(1)	1.456(4)	10(2)

[a] $U_{eq}=\frac{1}{3}\Sigma_i\Sigma_j U_{ij}a_i^* a_j^*$

5A forming a + *gauche* torsion angle with the carbon chain of the head group. The conformation of the sugar moieties is therefore the same as in *anti*- and *syn*-D-arabinose oxime [29], DL-arabinitol [30], both molecules in the asymmetric unit of D-arabinitol [31], and 1,2,3,4,5-penta-*O*-acetyl-D-arabinitol [32], respectively, 4-(D-*arabino*-tetritol-1-yl)-4-imidazolin-2-ylidene ammonium chloride [33], and 1-deoxy-1-nitro-D-arabinitol [34]. In contrast to this, the terminal hydroxyl group is orientated in a linear extension of the carbon

Table 6
Bond lengths and angles of **2** [a]

C-1–O-1	1.228(5)	C-1–C-2	1.545(7)
C-1–N	1.315(5)	C-2–O-2	1.416(7)
C-2–C-3	1.536(8)	C-3–O-3	1.429(9)
C-3–C-4	1.530(9)	C-4–O-4	1.432(9)
C-4–C-5	1.520(9)	C-5–O-5	1.414(8)
N–C-7	1.475(9)	C-7–C-8	1.508(9)
C-8–C-9	1.52(1)	C-9–C-10	1.511(9)
C-10–C-11	1.53(1)	C-11–C-12	1.52(1)
C-12–C-13	1.53(1)	C-13–C-14	1.51(1)
C-14–C-15	1.52(1)	C-15–C-16	1.53(1)
C-16–C-17	1.52(1)	C-17–C-18	1.52(1)
O-1–C-1–C-2	121.2(3)	O-1–C-1–N	124.3(4)
C-2–C-1–N	114.5(3)	C-1–C-2–O-2	107.9(4)
C-1–C-2–C-3	114.8(4)	O-2–C-2–C-3	112.7(5)
C-2–C-3–O-3	109.0(5)	C-2–C-3–C-4	114.7(5)
O-3–C-3–C-4	105.7(5)	C-3–C-4–O-4	106.4(5)
C-3–C-4–C-5	112.8(5)	O-4–C-4–C-5	110.5(5)
C-4–C-5–O-5	113.3(6)	C-1–N–C-7	120.2(4)
N–C-7–C-8	112.2(5)	C-7–C-8–C-9	110.1(5)
C-8–C-9–C-10	114.4(5)	C-9–C-10–C-11	112.6(5)
C-10–C-11–C-12	114.7(6)	C-11–C-12–C-13	113.4(6)
C-12–C-13–C-14	115.5(6)	C-13–C-14–C-15	113.5(6)
C-14–C-15–C-16	114.9(6)	C-15–C-16–C-17	112.4(6)
C-16–C-17–C-18	113.1(7)		

[a] In Å and °.

Table 7
Selected torsion angles in open-chain arabinose derivatives with two independent molecules in the asymmetric unit

Angle [a]	A [a]	A′	B	B′	C	C′
O-1–C-1–C-2–C-3	−65	101	−172.5(2)	−64.1(3)	−175.3(4)	−172.2(4)
C-1–C-2–C-3–C-4	179	−178	173.7(2)	175.4(2)	−178.1(4)	−173.4(4)
C-2–C-3–C-4–C-5	−178	−179	−175.6(2)	172.0(2)	−179.3(4)	179.0(4)
O-1–C-1–C-2–O-2	177	−11	63.6(3)	174.6(2)	63.9(5)	68.1(5)
O-2–C-2–C-3–O-3	54	52	57.8(2)	58.6(2)	59.1(6)	67.7(6)
O-3–C-3–C-4–O-4	−174	−177	−174.1(2)	168.9(2)	176.8(3)	177.2(4)
O-4–C-4–C-5–O-5	−58	−61	−57.8(3)	−63.1(2)	−66.1(5)	−60.4(6)
C-3–C-4–C-5–O-5	62	57	66.2(3)	56.3(3)	55.2(6)	58.1(6)
N–C-1–C-2–C-3	115	−78				
C-7–N–C-1–C-2	−180	179				
C-8–C-7–N–C-1	−119	−178				
C-9–C-8–C-7–N	−165	−72				
C-7–C-8–C-9–C-10	175	−173				
C-8–C-9–C-10–C-11	−179	171				
C-9–C-10–C-11–C-12	−179	−179				
C-10–C-11–C-12–C-13	178	179				
C-11–C-12–C-13–C-14	−179	−177				

A, *N*-(1-octyl)-D-arabinonamide (1st molecule); A′, *N*-(1-octyl)-D-arabinonamide (2nd molecule); B, D-arabinitol (1st molecule); B′, D-arabinitol (2nd molecule); C, 1,2,3,4,5-penta-*O*-acetyl-D-arabinitol (1st molecule); C′, 1,2,3,4,5-penta-*O*-acetyl-D-arabinitol (2nd molecule). [a] The data for molecule 1 and 2 of **1** are rounded to 1°.

chain in the crystal structures of 2-amino-3-methyl-5-(D-*arabino*-1,2,3,4-tetrahydroxybutyl) imidazolium chloride [35] and Ca D-arabinonate [36].

Whereas the two independent molecules of **1** show an identical conformation of the sugar group, their overall conformation is different; O-1 and O-2 are arranged *anti* to each other, whereas the torsion angle O-1A–C-1A–C-2A–O-2A is almost synperiplanar. Two − *gauche*

Table 8
Selected torsion angles of *ribo*-configured compounds

angle	A	B	C	D
C-1–C-2–C-3–C-4	74.7(6)	75(1)	74	90
C-2–C-3–C-4–C-5	177.0(5)	177(1)	176	179
O-1–C-1–C-2–O-2	7.7(6)	8(1)		
O-2–C-2–C-3–O-3	69.0(6)	69(1)	72	54
O-3–C-3–C-4–O-4	178.1(4)	178(1)	179	−178
O-4–C-4–C-5–O-5	−64.5(7)	−65(1)	−64	−67
C-3–C-4–C-5–O-5	54.4(8)	55(1)	59	55
N–C-1–C-2–C-3	63.9(5)	63(1)		
C-7–N–C-1–C-2	175.8(4)	175(1)		
C-8–C-7–N–C-1	−177.5(4)	−176(1)		
C-9–C-8–C-7–N	179.4(6)	179(1)		

A, **2**; B, *N*-(1-decyl)-D-ribonamide (DOHHIR) [a]; C, D-ribose diethyldithioacetal (DRETAC) [a]; D, D-ribose diphenyldithioacetal (RIBPTA10) [a]. [a] Reference code taken from the Cambridge Structural Database

Table 9
Hydrogen bonds in the crystal structure of **1**

(a) Geometrical data of the hydrogen bonds of the XPLOR-optimization

H	D–H	A	D···A	H···A	D–H···A	Symmetry operator for A
H-N1	0.98	O-2	2.67	2.13	113	*x,y,z*
H-N1	0.98	O-3A	2.90	2.26	121′	$1+x,y,z$
H-N1A	0.98	O-5	2.94	1.96	177	$-1+x,y,-1+z$
H-O2	0.98	O-1A	3.26	2.37	151	$1+x,y,z$
H-O2	0.98	O-3	2.72	2.01	127	*x,y,z*
H-O2A	0.99	O-1A	2.62	2.07	113	*x,y,z*
H-O2A	0.99	O-2	2.72	2.10	119	$-1+x,y,z$
H-O2A	0.99	O-3A	2.64	2.19	106	*x,y,z*
H-O3	0.98	O-2	2.79	1.87	155	$-1+x,y,z$
H-O3A	0.98	O-2A	2.80	1.84	165	$-1+x,y,z$
H-O4	0.97	O-4A	2.76	1.81	168	$1+x,y,1+z$
H-O4A	0.98	O-5A	2.69	1.78	152	$1+x,y,z$
H-O5	0.99	O-4	2.66	1.80	145	$-1+x,y,z$
H-O5A	0.97	O−1	2.74	1.80	162	$-1+x,y,-1+z$

(b) Intermolecular oxygen–oxygen distances < 3 Å

Atom 1	Atom 2	*D*	Symmetry operator for Atom 2	Compared with D-arabinitol
O-2	O-2A	2.72	$1+x,y,z$	–
O-2	O-3	2.79	$1+x,y,z$	←
O-3	O-1A	2.79	$1+x,y,z$	–
O-4	O-4A	2.76	$1+x,y,1+z$	–
O-4	O-5	2.66	$1+x,y,z$	←
O-2A	O-3A	2.80	$1+x,y,z$	→
O-4A	O-5A	2.69	$1+x,y,z$	→
O-5A	O-1	2.74	$-1+x,y,-1+z$	–

[a] –, There exists no analogous oxygen–oxygen pair in the crystal structure of D-arabinitol. An arrow, however, indicates the existence of such an atom pair and gives the direction of the hydrogen bond between the two oxygen atoms. The analogy does not hold for the symmetry operations.

bends are found along N–C-1–C-2–C-3 and N–C-7–C-8–C-9 in the second molecule, whereas the corresponding angles of the first molecule are in the + *anticlinal* and *antiperiplanar* range, respectively. Compound **1** therefore exhibits pronounced conformational isomorphism [37], unlike the two independent molecules observed in the crystal structure of *N*-(1-octyl)-D-talonamide, which adopt nearly identical conformations [12].

The molecular geometry and the numbering scheme of **2** are shown in Fig. 3. The C–C bond lengths of the head group are in the range from 1.520(9) to 1.545(7) Å with a mean value of 1.532 Å and from 1.508(9) to 1.53(1) Å in the dodecyl chain (mean value 1.519 Å). The C–O_{OH} bond lengths have a mean value of 1.422 Å and lie between 1.414(8) to 1.432(9) Å. The C–C–C bond-angles display a mean value of 113.8°, hence all geometrical data of the head group are comparable to the values found in the crystal structures of alditols [8]. Compounds **2** exhibits two extended-chain segments ranging from C-2 to C-5 and C-

Table 10
Hydrogen bonds in **2** and *N*-(1-decyl)-D-ribonamide [a]

H	D–H	A	D···A	H···A	D–H···A	Symmetry operator for A
H-O2	0.72(6)	O-4	2.737(8)	2.08(5)	152(5)	$x,-1+y,z$
	0.85	O-4	2.736(5	1.94	157	$x,1+y,z$
H-O3	0.83(6)	O-2	2.737(8)	1.93(5)	166(6)	$-1+x,y,z$
	0.62	O-2	2.741(5)	2.21	146	$-1+x,y,z$
H-O4	0.82(8)	O-5	2.740(8)	2.03(8)	146(7)	$1+x,y,z$
	0.82	O-5	2.742(5)	1.93	167	$1+x,y,z$
H-O5	0.88(7)	O-3	2.808(9)	2.01(6)	151(5)	$x,1+y,z$
	0.92	O-3	2.805(5)	1.98	150	$x,-1+y,z$
H-N	0.91	O-1	2.957(8)	2.16	146	$-1+x,y,z$
	0.86	O-1	2.977(5)	2.14	162	$-1+x,y,z$

[a] First row, dodecyl derivative; second row, decyl derivative.

2 to C-14, respectively. The torsion angle C-1–C-2–C-3–C-4 is 74.7(6)° causing a 1,3-syndiaxial interaction between the carbonyl carbon atom C-1 and O-4. This interaction is unexpected, since a bent conformation, free of 1,3-syn interactions, can be formulated for open-chain ribose derivatives. In fact, this sickle arrangement is realized in the crystal structure of another *ribo*-configured amphiphilic compound, namely 1-*O*-(β-D-glucopyranosyl)-D-*ribo*-3,4-dihydroxy-2-aminooctadecane hydrochloride monohydrate [38]. In contrast, compound **2** displaying the ${}_2G^+$ conformation is isostructural with its decyl homologue [39], both molecules in the asymmetric unit of the "pseudo"-enantiomer *N*-(1-octyl)-D-talonamide, D-ribose diethyl dithioacetal and its diphenyl homologue [40].

In contrast to that, open-chain ribose derivatives in solution usually exhibit a preference for the ${}_2G$ conformation, as has been reported for ribitol [41], *syn*-D-ribose oxime [42], and D-ribononitrile 2,3,4,5-tetraacetate [43,44], whereas D-ribose diethyl dithioacetal and its diphenyl homologue prefer a ${}_3G^+$ sickle conformation [40], since this conformation is the only form free of 1,3-syndiaxial interactions (compare Figs. 1a and 1b in Ref. [45]). With the former ribose derivatives, conformations that are extended from C-1 to C-5 contribute negligibly to the molecular population in solution, demonstrating that the different conformations are not isoenergetic. It must however be noted that conformations involving C//O- or C//C-interactions were explicitly precluded from the combined NMR–molecular mechanics investigation of the ribononitrile tetraacetate [43,44]. Additionally, a very recent 620-MHz high-field NMR study [46] revealed that the conformational flexibility of alditols in solution is more dependent on the solvent than was previously assumed. Since the ^{13}C and ^{1}H NMR data published for *N*-(1-decyl)-D-ribonamide [47] do not permit a conformational analysis, nothing is known about the conformational behaviour of the ribonamides in solution. Almost indentical ^{13}C NMR resonances of the head groups suggest at least that the octyl-, decyl-, and dodecyl-ribonamide behave identically in Me_2SO [48]. As a ${}_2G^-$ sickle Dreiding model of **2** actually does not exhibit any C//O- or O//O-interaction, it may be reasonably assumed (with all caveats) that this conformation is favoured in solution in the concentration range where NMR spectra are usually taken and where the molecules are believed not to interact with each other [49]. In the crystal structure of *N*-(1-dodecyl)-D-ribonamide, however, a molecular conformation of elevated free

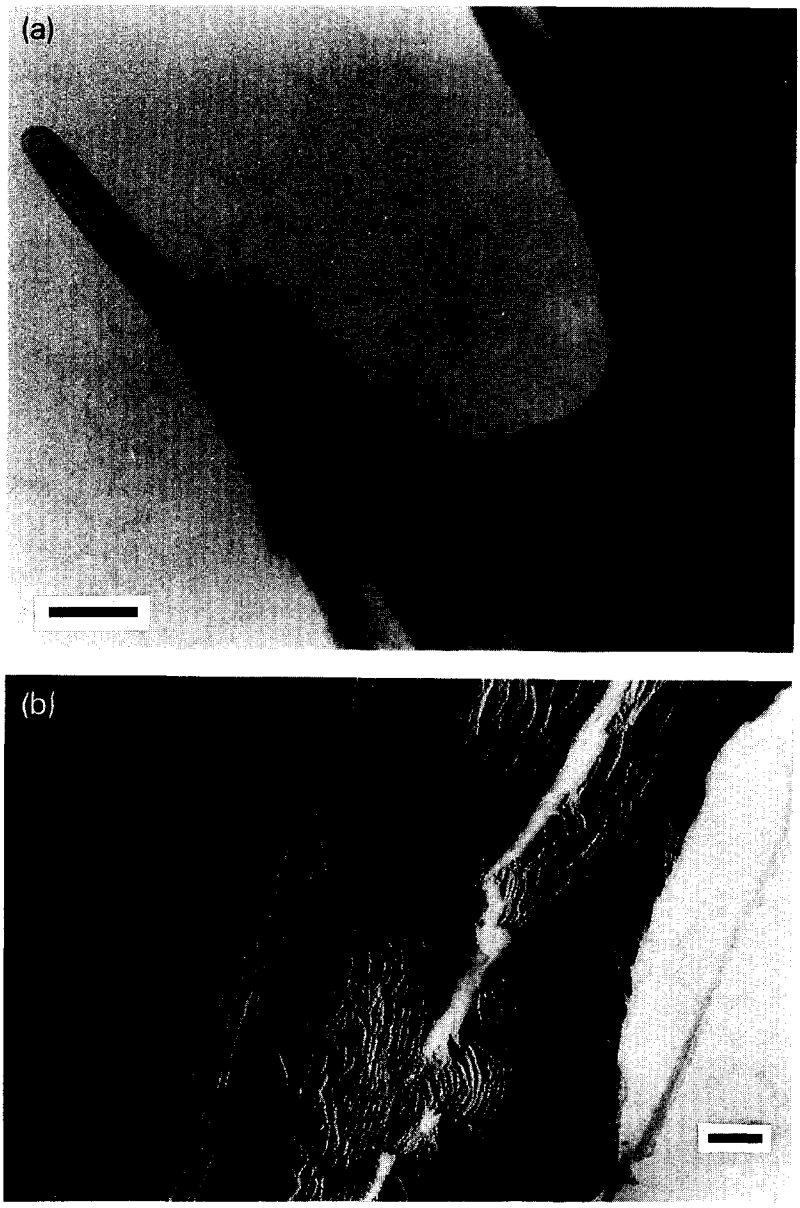

Fig. 1. (a) Tubules found for **1** in water (negatively stained, 2% phosphotungstate, pH 7). The black bar denotes 200 nm. (b) Molecular bilayer obtained from **3** in water. The bilayer thickness was measured by Pt-shadowing. The black bar corresponds to 200 nm.

energy (in the isolated state) is adopted as a consequence of intermolecular forces (see later).

Crystal packing.—As there is only one molecule in the unit cell of **2** (and its decyl homologue), the lattice translations generate a head-to-tail arrangement of the molecules

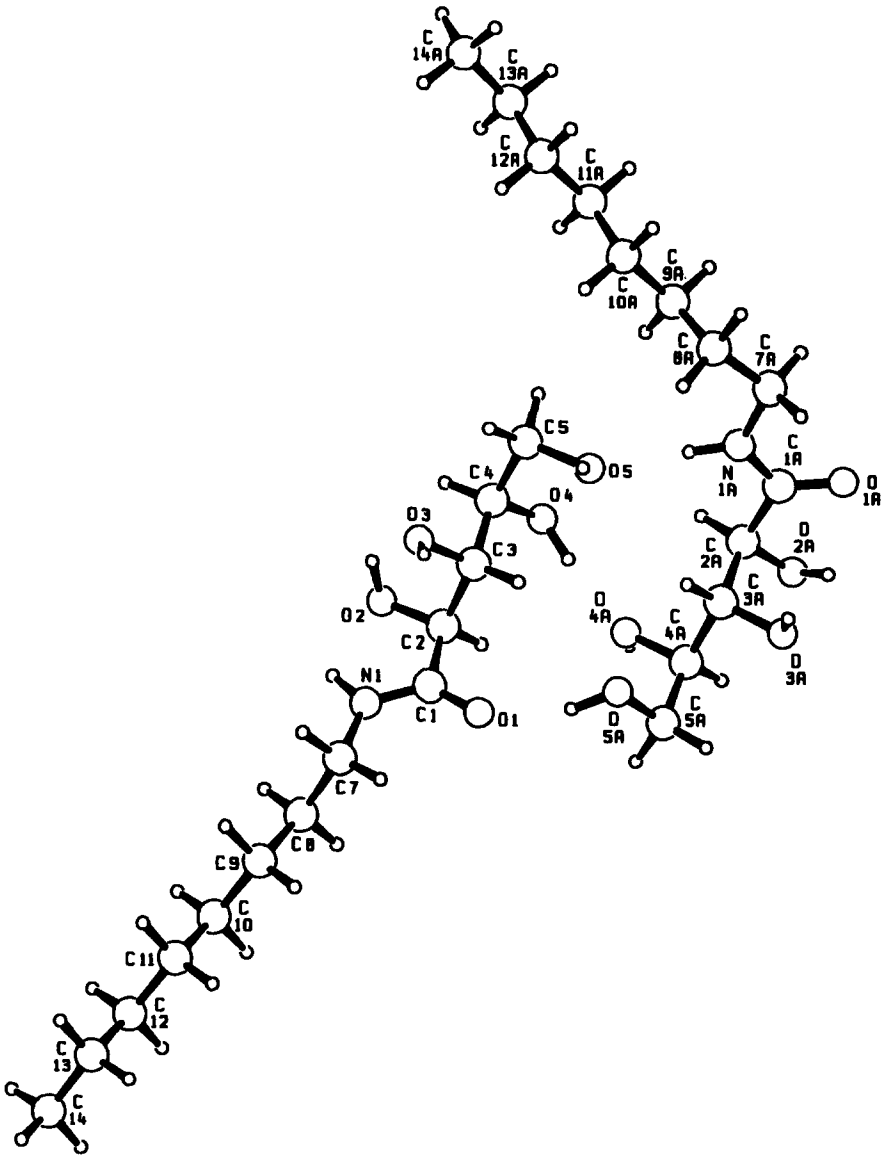

Fig. 2. Conformation and atomic numbering scheme of the two independent molecules of **1**.

in the crystal (Fig. 4). This packing pattern has also been observed in the crystal structures of *N*-(1-alkyl)- [50–52], *N*-alkanediyl-D-gluconamides [13,14], and the amphiphilic glucitol derivatives MEGA-9 [53] and MEGA-11 [54]. A head-to-head arrangement, as usually found for amphiphilic compounds, has been described for *N*-(1-octyl)-D-gulonamide [11] and the corresponding talose derivative [12]. Neither the head groups nor the alkyl tails are interdigitated in any of these crystal structures. In contrast, sugar amphipiles having cyclic head groups which crystallize with a head-to-head packing, also show inter-

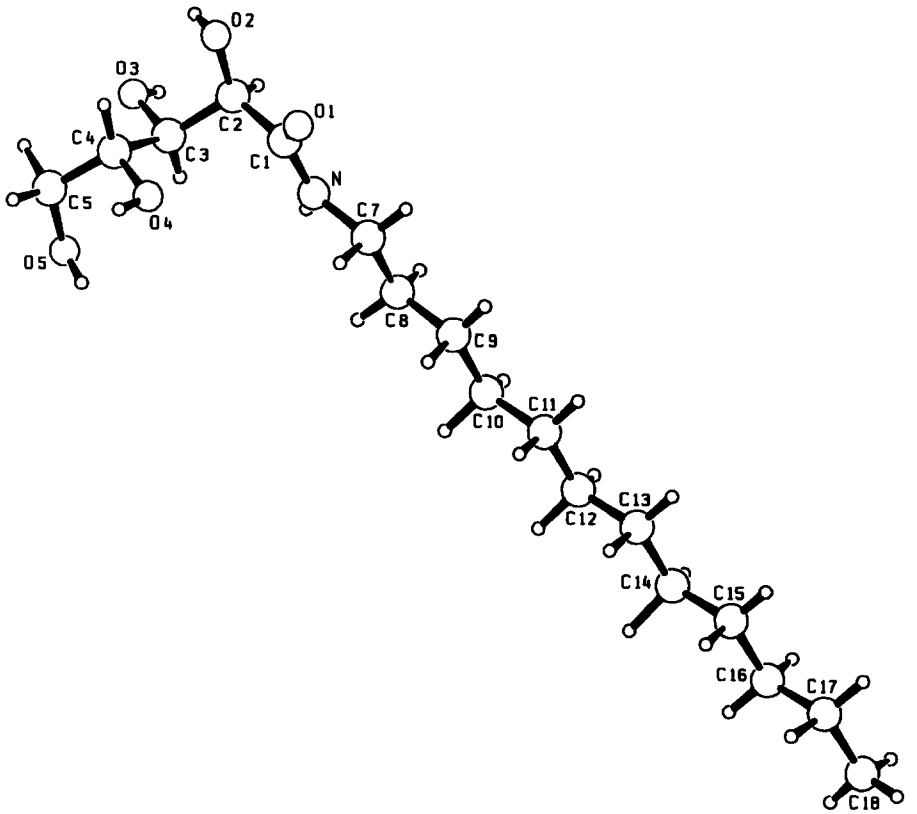

Fig. 3. Conformation and atomic numbering scheme of **2**.

calating alkyl chains (cf. Ref. [26] and references cited therein). This behaviour may also be observed in the crystal structures of pyridine [55], pyrimidinone [56], and piperazine [57] amphiphiles and is attributed to the voluminous head-group moieties. Their larger space requirements have to be compensated by interdigitation of the alkyl chains.

Compound **1**, exhibiting two independent molecules oriented in an antiparallel manner in its asymmetric unit, shows a packing mode that has never been observed with amphiphilic aldonamides: both the head groups and the hydrophobic tails are interdigitated (Fig. 5). The arrangement of the molecules is therefore identical with that of MEGA-8 [54] where the packing mode of the interdigitating head groups was falsely named as "head-to-head". In this crystal structure, the antiparallel orientation of the molecules is generated by the symmetry operations of the space group ($P2_12_12_1$) and not by two molecules aligned antiparallel as with **1**.

Hydrogen-bonding scheme. Endless spirals of hydrogen-bonding chains were proposed for the hydrogen-bonding schemes of D-ribose diethyl dithioacetal and its diphenyl homologue [58], whereas the hydrogen-bonding scheme of the amphiphilic ribonamides consisting of two distinct patterns is quite different. On the one hand, the amide hydrogen and oxygen atoms form endless hydrogen-bonding chains of the kind H···O=C–N–H···O=C···, etc., that are common to acyclic secondary amides (cf. footnote 17d in Ref. [59]). On the

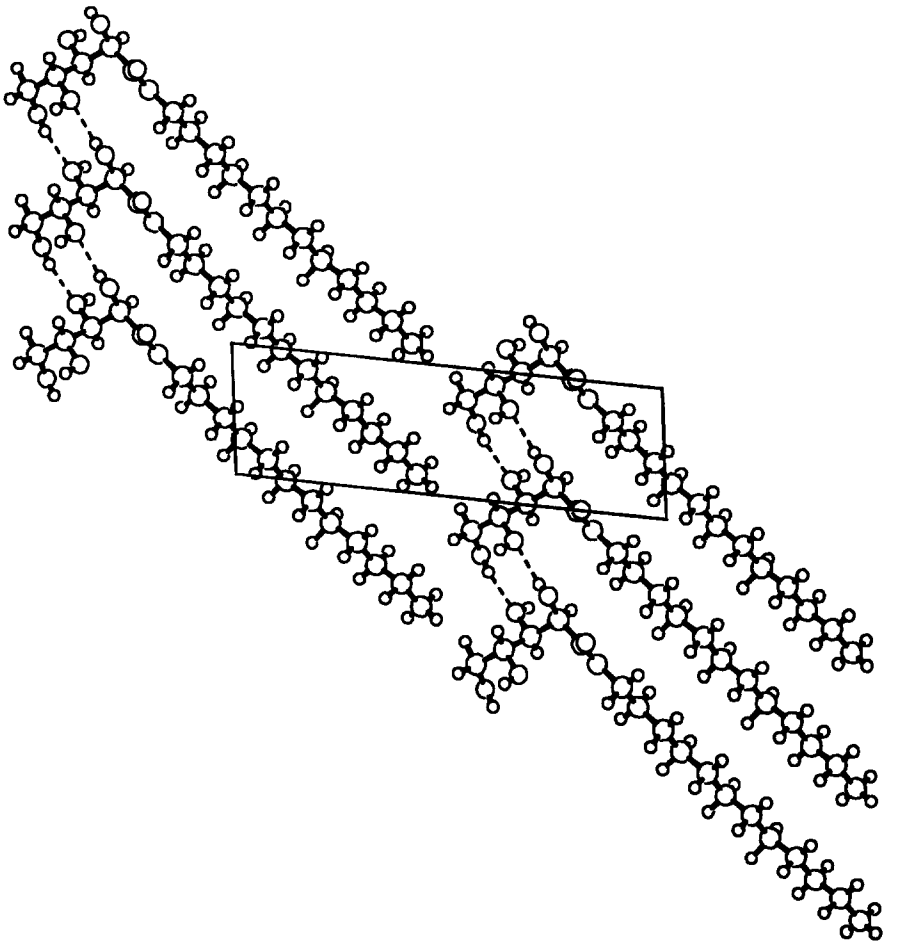

Fig. 4. Head-to-tail packing of **2**.

other hand, a quadrilateral, homodromic cycle [60] is formed by the hydroxyl groups on molecules that are related by lattice translations along the two ca. 5 Å long lattice constants (Fig. 6). This pattern has recently been found to be a general packing principle of different acyclic-sugar derivatives [61] and is also found in the crystal structures of amphiphilic open-chain glucose derivatives [62]. A special spatial arrangement of the hydroxyl groups on the sugar chain is needed for building up this cycle, as discussed in Ref. [61]. This special arrangement is accomplished in the ribonamides by a rotation around C-2 and C-3, thereby generating the 1,3-syn interaction between C-1 and O-4. The destabilization by this interaction is at least compensated by the gain in energy due to the homodromic cycle: the intermolecular interactions in the crystal therefore enforce the adoption of a conformation that is only observed with low occupancy in solution

As the positions of the hydroxyl hydrogen atoms in **1** were not taken from difference-Fourier maps, but are the result of the XPLOR-refinement, the hydrogen bonding scheme of **1** should not be discussed on the basis of this potential-energy calculation, but has to be

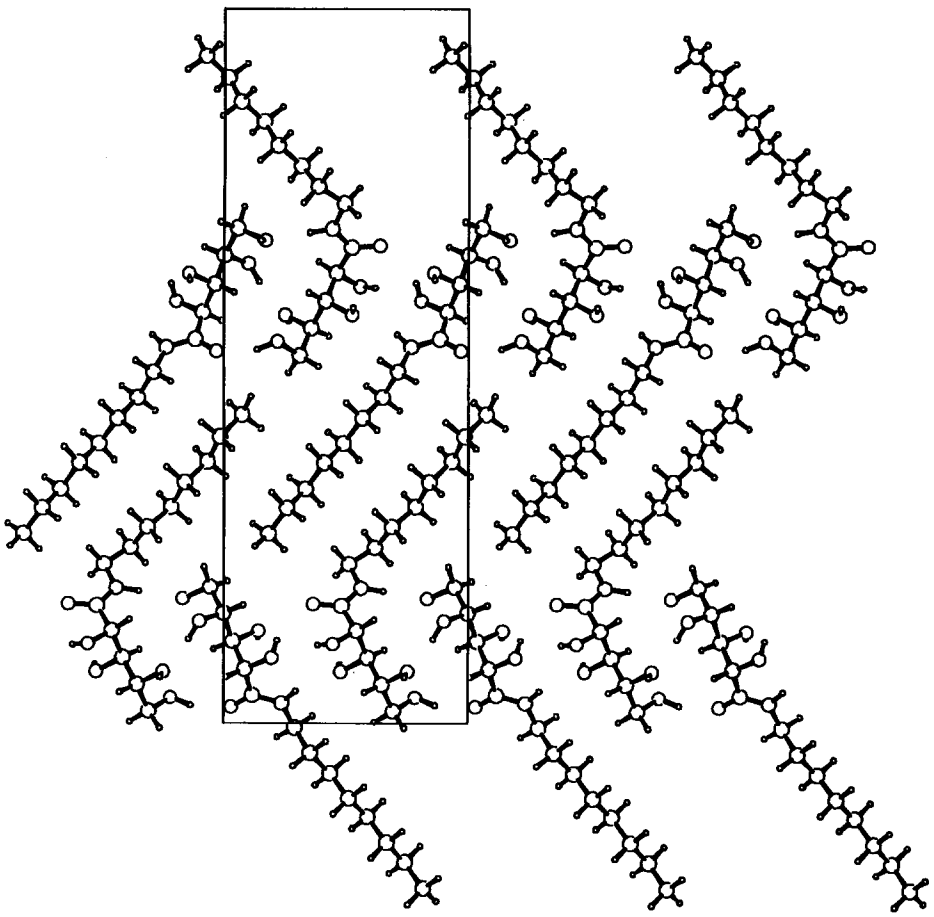

Fig. 5. Crystal packing of **1**, showing the intercalation both of the head groups and the alkyl tails.

derived from oxygen–oxygen distances below 3 Å; this does not rule out a comparison of the two schemes. The atoms of the amide bonds are not involved in endless H···O=C–N–

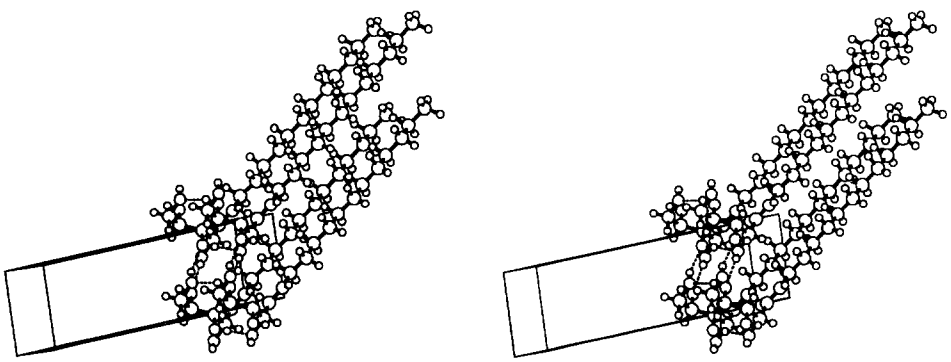

Fig. 6. Stereoplot of the homodromic quadrilateral hydrogen-bond cycle in the crystal structure of **2**.

H···O=C– chains as found in the crystal structures of *N*-(1-octyl)-D-glucon-, -gulon-, and -talonamide and of *N*-(1-dodecyl)-D-ribonamide. N-1 forms an almost planar (sum of angles = 346°) bifurcated hydrogen bond with an intramolecular branch to O-2 and an intermolecular bond to O-3$A_{1+x,y,z}$. N-1A, however, does not form an intramolecular hydrogen bond with O-2A because of the conformational differences of the two molecules. It is a donator of a linear hydrogen bond to the terminal hydroxyl group O-5 of a neighbouring molecule that is oriented in an antiparallel fashion. Formulating a cooperative hydrogen-bonding pattern on the basis of intermolecular oxygen–oxygen distances and the data of the amide protons given in Table 7 reveals a finite chain N-1$A_{x,y,z}$ → O-5$_{-1+x,y,-1+z}$ → O-4$_{-2+x,y,-1+z}$ → O-4$A_{-1+x,y,z}$ → O-5$A_{x,y,z}$ → O-1$_{-1+x,y,-1+z}$ that is identical with the hydrogen-bonding pattern optimized by XPLOR for these atoms. A second chain may be formulated on the basis of intermolecular distances, namely N-1 → O-3$A_{1+x,y,z}$ → O-2$A_{x,y,z}$ → O-2$_{-1+x,y,z}$ → O-3$_{x,y,z}$ → O-1$A_{1+x,y,z}$. This pattern, however, is in contradiction to the XPLOR-hydrogen-bonding scheme which includes bifurcated and trifurcated hydrogen bonds, donated by O-2 and O-2A, respectively. It is impossible, therefore, to give the detailed hydrogen-bonding scheme of **1** on the basis of the existing data. However, a quadrilateral homodromic cycle of general connectivity O-2···O-4···O-5···O-3 as found in the crystal structures of *anti*-D-arabinose oxime [29,61] and 1-deoxy-1-nitro-D-*arabino*-pentitol [34,61] may definitively be precluded for **1**. Two independent molecules form the asymmetric unit of **1** and its lattice constants display only one ca. 5 Å long axis. These factors are incompatible with a cycle of this special connectivity, as pointed out recently [61].

D-Arabinitol exhibits, like **1**, two independent molecules oriented in an antiparallel manner and the intermolecular oxygen–oxygen distances of all unambigously determined hydrogen-bonds in that structure are shorter than 3 Å. A comparison betweeen **1** and D-arabinitol could therefore provide additional insights. The hydrogen-bonding scheme of D-arabinitol consists of only one hydrogen-bond chain in which all hydroxyl groups are involved. This was not mentioned in the original publication. However, as can be seen in Table 9, there are only a few oxygen–oxygen pairs that are identical both in **1** and D-arabinitol; a similarity of the hydrogen-bonding patterns between these compounds, therefore, is not observed.

There is, however, a significant agreement of parts of the hydrogen-bonding schemes of **1** and MEGA-8, as shown in Scheme 2. Short chains are found in both crystal structures: they run from the preterminal to the terminal hydroxyl group of a neigbouring molecule in parallel arrangement. The latter hydroxyl group then donates a hydrogen atom to the carbonyl oxygen atom of a neighbouring molecule that is oriented in antiparallel manner. Both crystal structures therefore display a hydrogen bond between the terminal hydroxyl group and the carbonyl oxygen atom of a molecule in antiparallel arrangement, and this links the interdigitated head groups together.

Similar observations have been made in the crystal structures of 1,4-dimethyl-3-(D-*galacto*-pentitol-1-yl)-5-(*p*-tolyl)pyrazole [63] and 4,6-diamino-5-octylpyrimidine-2(1*H*)-one [56], where molecules in antiparallel arrangement are also found. Hydrogen bonds derived from intermolecular oxygen–nitrogen distances can again be formulated in these structures which interlock molecules oriented in a manner comparable to **1** and MEGA-8, namely between the outer and the most inner hydrophilic functional-group of molecules in antiparallel arrangement.

N-(1-octyl)-D-arabinonamide

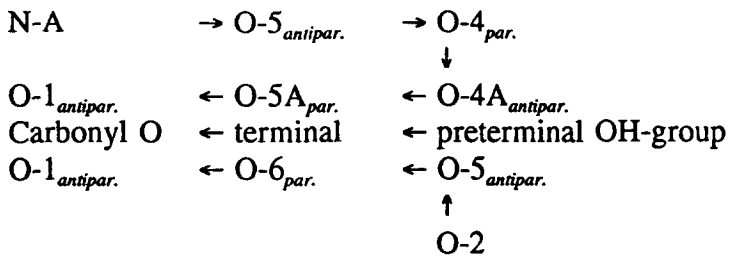

MEGA-8 [1-deoxy-(*N*-methyloctanamido)-D-glucitol]

Scheme 2. Parts of the hydrogen-bonding schemes of **1** and MEGA-8 as derived from intermolecular oxygen–oxygen distances (**1**) and refined hydrogen positions (MEGA-8), respectively.

It is noteworthy that similar crystalline behaviour is found not only with acyclic sugar derivatives (namely related compounds), but also between members of differrent classes of compounds. A sketchy image of the crystallization process of these compounds emerges on the basis of this observation. It seems likely that the common pattern, namely interdigitated head-groups in antiparallel arrangement, is formed at an early stage of the crystallization process [64,65] when solute–solvent interactions have to be replaced by intersolute interactions because of the lower availability of the solvent. The interactions in such clusters requires satisfaction of the hydrogen-bonding properties of the functional groups of these compounds. In the case of **1**, MEGA-8, and 1,4-dimethyl-3-(D-*galacto*-pentitol-1-yl)-5-(*p*-tolyl)pyrazole, this saturation of the hydrogen bonds can be accomplished within the clusters, with the terminal hydroxyl groups still interacting with the solvent. These solvent molecules are expelled in a later step of crystallization when the terminal hydroxyl groups form a hydrogen bond with an acceptor on a molecule in antiparallel arrangement. Their more hydrophobic methylene groups become exposed and interact with the terminal methyl group of another molecule, thereby generating the intercalation of the alkyl chains.

However, as there is an amino group with *two* protons in the self-complementary 4,6-diamino-5-octylpyrimidine-2(1*H*)-one only *one* of which can make a hydrogen bond to a neigbouring molecule, the involvement of solvent molecules in the hydrogen-bonding scheme of the crystallization nuclei *and* the final crystal structure is necessary so that they are not expelled as crystallization proceeds. In fact, *N*,*N*-dimethylformamide molecules accepting a hydrogen bond from the second amino proton are contained in the cavity of the (nonintercalating) alkyl chains in the crystal structure of this pyrimidinone ampiphile. This structure, therefore, offers a "snapshot" of the *early* crystal nucleation sites supporting the general considerations made here for amphiphiles crystallizing in the less-common antiparallel arrangement.

Acknowledgements

This work was supported by the Sonderforschungsbereich 312 "Gerichtete Membranprozesse" of the Deutsche Forschungsgemeinschaft, the Förderkommission of the Freie

Universität Berlin, the Graduiertenkolleg "Synthese und Strukturaufklärung niedermolekularer Verbindungen", and the Fonds der Chemischen Industrie.

References

[1] B. Pfannemüller and W. Welte, *Chem. Phys. Lipids*, 37 (1985) 227–240.
[2] J.-H. Fuhrhop, S. Svenson, C. Boettcher, E. Rössler, and H.-M. Vieth, *J. Am. Chem. Soc.*, 112 (1990) 4307–4312.
[3] J.-H. Fuhrhop, P. Schnieder, J. Rosenberg, and E. Boekema, *J. Am. Chem. Soc.*, 109 (1987) 3387–3390.
[4] J.-H. Fuhrhop and C. Boettcher, *J. Am. Chem. Soc.*, 112 (1990) 1768–1776.
[5] J.-H. Fuhrhop, P. Schnieder, E. Boekema, and W. Helfrich, *J. Am. Chem. Soc.*, 110 (1988) 2861–2829.
[6] J.-H. Fuhrhop, S. Svenson, P. Luger, and C. André, *Supramolec. Chem.*, 2 (1993) 157–171.
[7] F.R. Taravel and B. Pfannemüller, *Makromol. Chem.*, 191 (1990) 3097–3106.
[8] G.A. Jeffrey and H.S. Kim, *Carbohydr. Res.*, 14 (1970) 207–216.
[9] G.A. Jeffrey, *Acta Crystallogr., Sect. B*, 46 (1990) 89–103.
[10] P. Köll, M. Morf, B. Zimmer, J. Kopf, A. Berger, K. Dax, and A.E. Stütz, *Carbohydr. Res.*, 242 (1993) 21–28.
[11] C. André, P. Luger, S. Svenson, and J.-H. Fuhrhop, *Carbohydr. Res.*, 230 (1992) 31–40.
[12] C. André, P. Luger, S. Svenson, and J.-H. Fuhrhop, *Carbohydr. Res.*, 240 1993) 47–56.
[13] J.-H. Fuhrhop, P. Blumtritt, C. Lehmann, and P. Luger, *J. Am. Chem. Soc.*, 113 (1991) 7437–7439.
[14] C. André, P. Luger, and J.-H. Fuhrhop, *Chem. Phys. Lipids*, 71 (1994) 175–186.
[15] C. André, P. Luger, D. Nehmzow, and J.-H. Fuhrhop, *Carbohydr. Res.*, 261 (1994) 1–11.
[16] A. Müller-Fahrnow, R. Hilgenfeld, H. Hesse, W. Saenger, and G. Pflügl, *Biochim. Biophys. Acta*, 978 (1989) 176–178.
[17] A.M. Connell and I. Pascher, *Acta Crystallogr., Sect. B*, 25 (1969) 2553–2561.
[18] H.S. Isbell and H.L. Frush, *Bur. Stand. U.S. J Res.*, 6 (1931) 1195; *Chem. Abstr.*, 28 (1934) 7263.
[19] G.M. Sheldrick, in G.M. Sheldrick, C. Krüger, and R. Goddard (Eds.), *Crystallographic Computing* 3, Oxford University Press, Oxford, 1985, pp 175–189.
[20] S.R. Hall and J.M. Stewart (Eds.), XTAL 2.2 Users Manual, University of Western Australia, Australia and Maryland, USA, 1987.
[21] C.G. Gilmore, MITHRIL, University of Glasgow, Scotland, 1983.
[22] A. Brünger, XPLOR 3.0, The Howard Hughes Medical Institute and Department of Molecular Biophysics and Biochemistry, Yale University, New Haven, USA, 1992.
[23] A. Brünger, M. Karplus, and G.A. Petsko, *Acta Crystallogr., Sect. A*, 45 (1989) 50–61.
[24] S. Kirkpatrick, C.D. Gelatt, Jr., and M.P. Vecchi, *Science*, 220 (1983) 671–680.
[25] T. Kunitake, Y. Okahata, M. Shimomura, S. Yasunami, and K. Takarabe, *J. Am. Chem. Soc.* 103 (1981) 5401–5413.
[26] G.A. Jeffrey and L.M. Wingert, *Liq. Cryst.*, 12 (1992) 179–202.
[27] D. Baeyens-Volant, R. Fornasier, E. Szalai and C. David, *Mol. Cryst. Liq. Cryst.*, 135 (1986) 93–110.
[28] D. Baeyens-Volant, P. Cuvelier, R. Fornasier, E. Szalai and C. David, *Mol. Cryst. Liq. Cryst.*, 128 (1985) 277–286.
[29] A. Mostad, *Acta Chem Scand. Sect. B*, 32 (1978) 733–742.
[30] F.D. Hunter and R.D. Rosenstein, *Acta Crystallogr. Sect. B*, 24 (1968) 1652–1660.
[31] J. Kopf, M. Morf, B. Zimmer, and P. Köll, *Carbohydr. Res.*, 218 (1991) 9–13.
[32] J. Kopf, M. Morf, B. Zimmer, and P. Köll, *Carbohydr. Res.*, 233 (1992) 35–43.
[33] A. Lopez-Castro, R. Vega, J. Fernandez-Bolanos, and M. Barragan, *Carbohydr. Res.*, 187 (1989) 139–144.
[34] J. Kopf, H. Brandenburg, W. Seelhorst, and P. Köll, *Carbohydr. Res.*, 200 (1990) 339–354.
[35] R. Vega, A. Lopez-Castro, and R. Marquez, *Acta Crystallogr. Sect. C*, 44 (1988), 156–159.
[36] S. Furberg and S. Helland, *Acta Chem. Scand.*, 16 (1962) 2373–2383.
[37] J. Bernstein, in G.R. Desiraju (Ed.), *Organic Solid State Chemistry*, Elsevier, Amsterdam, 1987, pp 471–518.
[38] S. Abrahamsson, B. Dahlén, and I. Pascher, *Acta Crystallogr., Sect. B*, 33 (1977) 2008–2013.

[39] B. Tinant, J.P. Declercq, and M. Van Meerssche, *Acta Crystallogr., Sect. C*, 42 (1986) 579–581.
[40] A. Ducruix, D. Horton, C. Pascard, J.D. Wander, and T. Prangé, *J. Chem. Res. (S)*, (1978) 470–471.
[41] G.E. Hawkes and D. Lewis, *J. Chem. Soc., Perkin Trans.* 2, (1984) 2073–2078.
[42] J.R. Snyder, *Carbohydr. Res.*, 198 (1990) 1–13.
[43] F. Lopez-Calahorra, D. Velasco, J. Castells, and C. Jaime, *J. Org. Chem.*, 55 (1990) 3526–3530.
[44] F. Lopez-Calahorra, D. Velasco, J. Castells, and C. Jaime, *J. Org. Chem.*, 55 (1990) 3530–3536.
[45] D. Horton and D. Wander, *J. Org. Chem.*, 39 (1974) 1859–1863.
[46] F. Franks, J. Dadok, S. Ying, R.L. Kay, and J.P. Grigera, *J. Chem. Soc., Faraday Trans.*, 87 (1991) 579–585.
[47] D. Baeyens-Volant, P. Cuvelier, R. Fornasier, E. Szalai, and C. David, *Mol. Cryst. Liq. Cryst.*, 128 (1985) 277–286.
[48] D. Baeyens-Volant, R. Fornasier, E. Szalai, and C. David, *Mol. Cryst. Liq. Cryst.*, 135 (1986) 93–110.
[49] D. Horton, Z. Wałaszek, and I. Ekiel, *Carbohydr. Res.*, 119 (1983) 263–268.
[50] V. Zabel, A. Müller-Fahrnow, R. Hilgenfeld, W. Saenger, B. Pfannemüller, V. Enkelmann, and W. Welte, *Chem. Phys. Lipids*, 39 (1986) 313–327.
[51] A. Müller-Fahrnow, R. Hilgenfeld, H. Hesse, W. Saenger, and B. Pfannemüller, *Carbohydr. Res.*, 176 (1988) 165–174.
[52] G.A. Jeffrey and H. Maluszynska, *Carbohydr. Res.*, 207 (1990), 211–219.
[53] A. Müller-Fahrnow, V. Zabel, M. Steifa, and R. Hilgenfeld, *J. Chem. Soc., Chem. Commun.*, (1986) 1573–1574.
[54] G.A. Jeffrey and H. Maluszynska, *Acta Crystallogr., Sect. B*, 45 (1989) 447–452.
[55] H.H. Paradies and F. Habben, *Acta Crystallogr., Sect. C*, 49 (1993) 744–747.
[56] J.M. Lehn, M. Mascal, A. DeCian, and J. Fischer, *J. Chem. Soc., Perkin Trans.* 2, (1992) 461–467.
[57] L. Venkatrami and B.M. Craven, *Acta Crystallogr., Sect. C*, 47 (1991) 968–875.
[58] A. Ducruix, D. Horton, C. Pascard, J.D. Wander, and T. Prangé, *J. Chem. Res. (M)*, (1978) 5438–5450.
[59] M. Etter, *Acc. Chem. Res.*, 23 (1990) 120–126.
[60] W. Saenger, *Nature*, 279 (1979) 343–344.
[61] C. André, P. Luger, B. Rosengarten, and J.-H. Fuhrhop, *Acta Crystallogr., Sect. B*, 49 (1993) 375–382.
[62] G.A. Jeffrey, *Mol. Cryst. Liq. Cryst.*, 185 (1990) 209–213.
[63] M.D. Estrada De Oya and A. Lopez-Castro, *Carbohydr. Res.*, 219 (1991) 215–222.
[64] M.C. Etter, J.C. MaCDonald, and J. Bernstein, *Acta Crystallogr., Sect. B*, 46 (1990) 256–262.
[65] F.H. Allen, S. Bellard, M.D. Brice, B.A. Cartwright, A. Doubleday, H. Higgs, T. Hummelink, B.G. Hummelink-Peters, O. Kennard, W.D. Motherwell, J.R. Rodgers, and D.G. Watson, *Acta Crystallogr., Sect B*, (1979) 2331–2339.